Acta Neuropathol (1992) 84: 559 – 569

Acta Neuropathologica
© Springer-Verlag 1992

Ultrastructural features of spongiform encephalopathy transmitted to mice from three species of bovidae

M. Jeffrey[1], J. R. Scott[2], A. Williams[2], and H. Fraser[2]

[1] Lasswade Veterinary Laboratory, Bush Estate, Penicuik, Midlothian EH26 OSA, UK
[2] AFRC and MRC Neuropathogenesis Unit, Institute for Animal Health, West Mains Road, Edinburgh, EH9 3JF, UK

Received February 3, 1992/Accepted May 18, 1992

Summary. The ultrastructural neuropathology of mice experimentally inoculated with brain tissue of nyala (*Tragelaphus angasi;* subfamily *Bovinae*), or kudu (*Tragelaphus strepsiceros;* subfamily *Bovinae*) affected with spongiform encephalopathy was compared with that of mice inoculated with brain tissue from cows (*Bos taurus;* subfamily *Bovinae*) with bovine spongiform encephalopathy (BSE). As fresh brain tissue was not available for nyala or kudu, formalin-fixed tissues were used for transmission from these species. The effect of formalin fixation was compared with that of fresh brain in mice inoculated with fixed and unfixed brain tissue from cows with BSE. The nature and distribution of the pathological changes were similar irrespective of the source of inoculum or whether the inoculum was from fresh or previously fixed tissue. Vacuolation caused by loss of organelles and swelling was present in dendrites and axon terminals. Vacuoles were also seen as double-membrane-bound and single-membrane-bound structures within myelinated fibres, axon terminals and dendrites. Vacuoles are considered to have more than one morphogenesis but the structure of vacuoles in this study was nevertheless similar to previous descriptions of spongiform change in naturally occurring and experimental scrapie, Creutzfeldt-Jakob disease, Gerstmann-Sträussler-Scheinker syndrome and kuru. Other features of the ultrastructural pathology of the transmissible spongiform encephalopathies including dystrophic neurites and scrapie-associated particles or tubulovesicular bodies were also found in this study. Neuronal autophagy was a conspicuous finding. It is suggested that excess prion protein (PrP) accumulation, or accumulation of the scrapie-associated protease-resistant isoform of PrP, may lead to localised sequestration and phagocytosis of neuronal cytoplasm and ultimately to neuronal loss.

Correspondence to: M. Jeffrey (address see above)

Key words: Neuronal autophagy – Bovine spongiform encephalopathy – Lysosomes – Ultrastructure – Vacuolation

Bovine spongiform encephalopathy (BSE) is a recently recognised member of the group of transmissible spongiform encephalopathies [12, 37] caused by novel but as yet incompletely characterised agents. As well as cattle, five exotic bovid species kept in zoological and wildlife park collections in Britain have developed a spongiform encephalopathy [10, 15, 22].

This study describes the ultrastructural pathology of a murine model of BSE. The purpose of the study was to compare the ultrastructural pathological findings in mice infected with BSE from three different bovine sources with those of previously published accounts of ultrastructural features of scrapie, kuru, Creutzfeldt-Jakob disease (CJD) and Gerstmann-Sträussler-Scheinker syndrome. As fresh brain tissue was not available from nyala and kudu for transmission of disease to mice, formalin-fixed tissues were used. The effect of formalin-fixed brain tissue was compared with that of fresh brain in mice inoculated with fixed and unfixed brain tissue from cows with BSE.

Materials and methods

Eight mice were selected for electron microscopy studies from four larger groups of RIII/FaDk mice which had been intracerebrally (0.02 ml) and intraperitoneally (0.1 ml) inoculated with unspun 10% brain homogenate from one of four sources. Two of these mice had been inoculated with fresh brain from a cow with BSE, two with formalin-fixed BSE brain, two with formalin-fixed kudu brain and two with formalin-fixed nyala brain. Prior to inoculation, formalin-fixed brain tissue was homogenised after the formalin had been leached out in distilled water overnight. (Detailed case histories of the nyala and kudu have been published previously [17, 22].) A further four age-matched, uninjected RIII/FaDk mice were available as controls (Table 1). Details of experimental protocols and results of these experiments are the subject of a separate paper (Fraser et al., in preparation).

Table 1. The distribution of vacuolation and autophagy by light and electron microscopy[a]

Animal No. and source of inoculum	Site of vacuolation							
	Cochlear nucleus (a)	Paraterminal body (b)	Cerebellar white matter (c)	Dorsal medulla (d)	Dorsal lateral geniculate (e)	Superior colliculus (f)	Occipital cortex (g)	Autophagy Anatomic location (a–g)
1 Cow BSE unfixed	+++	+	++	+++	+	++	+	b, f
2 Cow BSE unfixed	+++	+	++	+++	−	+	+	f
5 Cow BSE formal fixed	+++	+	++	+++	+	++	+	b, e, f
6 Cow BSE formal fixed	+++	+	++	+++	−	+	+/−	d, e, f
3 Nyala formal fixed	+++	+	+	+++	+	++	−	e, f
4 Nyala formal fixed	+++	+	++	+++	+/−	+	+/−	b, d, f, g
10 Kudu formal fixed	+++	+	++	+++	+	+	−	a, b, d, f
12 Kudu formal fixed	+++	+	++	+++	+/−	++	−	b, d, f
7 Control	−	−	−	−	−	+/−	+/−	−
8 Control	+/−	−	−	−	−	−	−	−
9 Control	−	−	−	−	−	−	−	−
11 Control	−	−	−	−	−	−	−	−

[a] These results were obtained by blind examination of coded sections and grids
− none, +/− trace, + mild, ++ moderate, +++ severe vacuolation

All the experimentally inoculated mice used in the above-mentioned studies developed neurological illness with incubation periods between 300–400 days. Mice were killed by intracardiac perfusion under chloral hydrate anaesthesia with 100 ml of 2.5 % glutaraldehyde and 2 % paraformaldehyde in cacodylate buffer at room temperature. Brains were left in situ overnight and were then removed to cacodylate buffer. Samples of tissue were taken from the dorsal medulla, cochlear nucleus, dorsal lateral geniculate nucleus, parietal cortex, superior colliculus, paraterminal body and cerebellar white matter. Tissues were post-fixed in osmium tetroxide, dehydrated and embedded in araldite and coded by an independent assistant. Semithin sections were stained with toluidine blue and ultrathin sections from selected areas were mounted on nickel grids and were examined using a Jeol 100B or a Hitachi H600 electron microscope.

Results

Controls

Light microscopy. Occasional holes, (not considered to be dilated capillaries), were recorded as sparse vacuoles at some sites in some mice (Table 1).

Electron microscopy. Occasional swollen astrocytic processes, located around otherwise normal blood vessels and neuronal intranuclear vacuoles were present in control tissues. Rarely dendrites were swollen and showed a decrease in numbers or density of subcellular organelles. Wallerian-type degeneration of myelinated axons and so-called dystrophic neurites, mostly of the kind designated type 1 [27], consisting of numerous pleomorphic membrane-bound electron-dense inclusions, were also an infrequent finding (Fig. 1a). From one to four large vacuoles were seen at each site examined in each control mouse. Vacuoles of up to 40-μm diameter were present in both myelinated (Fig. 1b) and unmyelinated processes. Small irregularly shaped single-membrane-bound vacuoles, thought to arise from smooth endoplasmic reticulum (SER), were occasionally found in neuronal and glial perikarya, in glial cell processes and in axons and dendrites (Fig. 1c). Rarely, such vacuoles occupied almost the entire diameter of a neurite (Fig. 1c).

Inoculated mice

Light microscopy. Examination of toluidine blue-stained sections confirmed lesions of spongiform encephalopa-

Fig. 1a–c. Features seen in control mice. **a** Dystrophic neurite containing numerous pleomorphic membrane-bound bodies containing membranous or amorphous electron-dense material. × 37,000. **b** Vacuole in a myelinated fibre. The vacuole is probably located between the axon plasmalemma and the myelin sheath. × 37,000. **c** Single-membrane-bound vacuole present in a neurite. Surrounding neuropil is well preserved. Cysterns of dilated smooth endoplasmic reticulum (SER) are also present (*arrowheads*). × 7,500

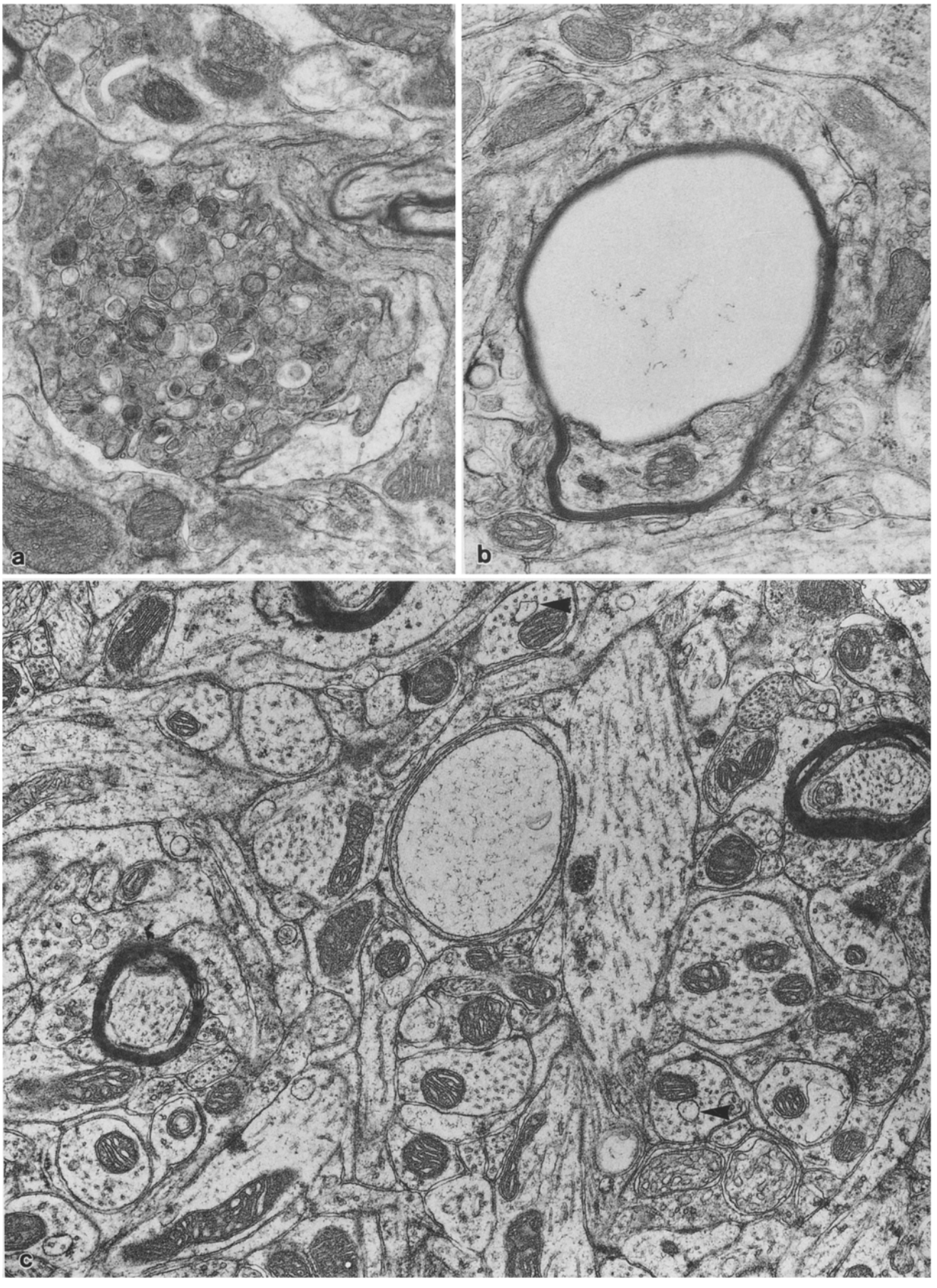
a
b
c

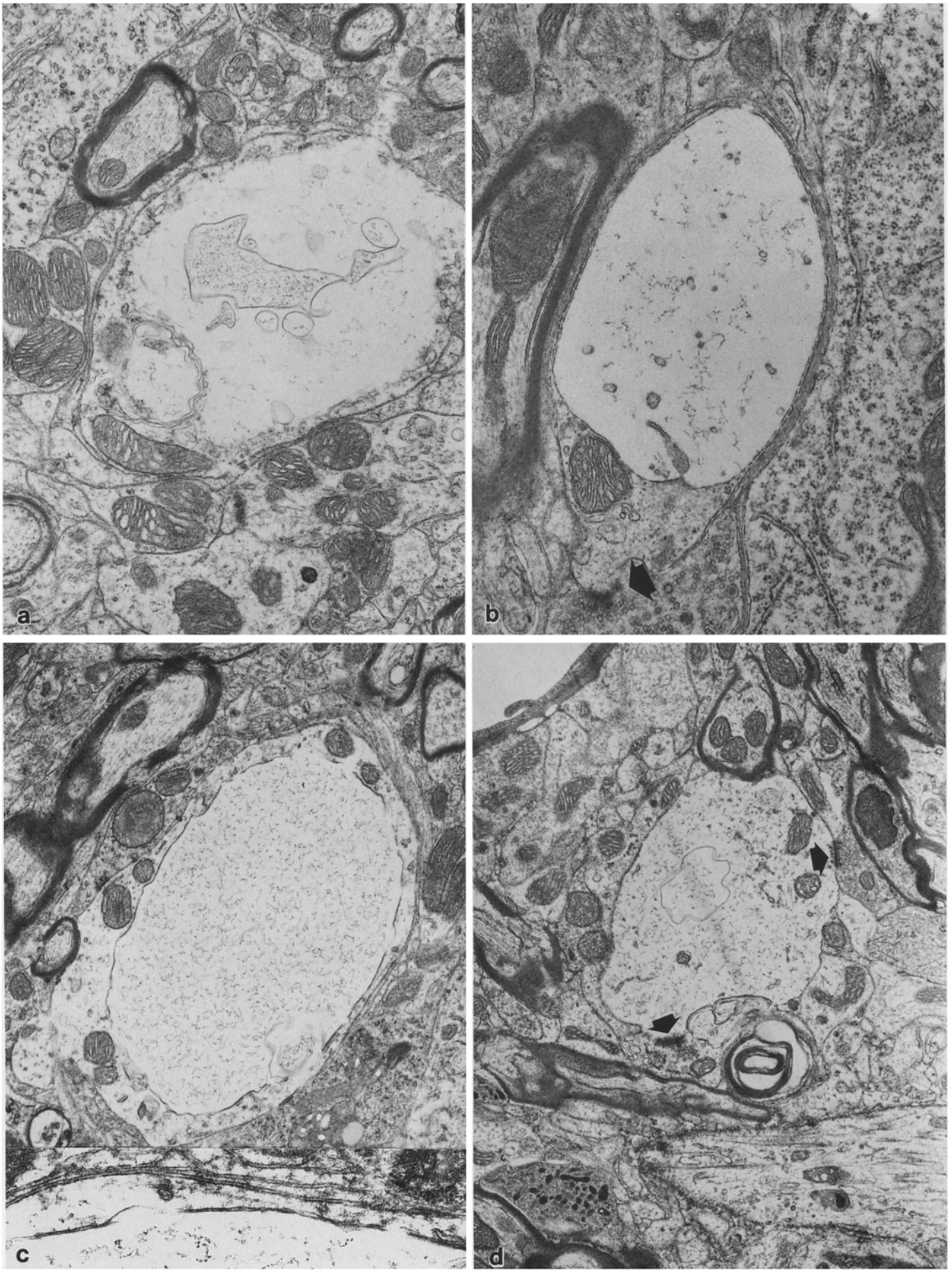

Fig. 2a–d

Fig. 2a–e. Vacuoles of dendrites. **a** Mouse inoculated with formalin-fixed nyala brain. Dendrite showing non-membrane-bound vacuole containing membranous debris. × 10,000. **b** Mouse inoculated with formalin-fixed kudu brain. Postsynaptic dendrite with single-membrane-bound vacuole containing granular and vesicular debris. The limiting membrane shows many small interruptions. *Arrow* shows synapse. × 30,000. **c** Mouse inoculated with fresh cow bovine spongiform encephalopathy (BSE) brain. Presumed dendrite with interrupted double-membrane-bound vacuole containing granular debris. × 10,000. *Inset:* Detail of limiting membrane of vacuole. × 40,000. **d** Mouse inoculated with formalin-fixed cow BSE brain. Postsynaptic dendrite with marked depletion of microtubules. *Arrows* indicate synapses. A dilated cystern of SER is also present. × 7,500. **e** Mouse inoculated with formalin-fixed cow BSE brain. A vacuole consisting of a distended process, probably a dendrite, shows no recognisable organelles, only granular debris. There is herniation of adjacent cell membranes into the vacuole. × 22,000

Fig. 3a, b. Vacuole and vacuole-like structures in axon terminals. **a** Mouse inoculated with formalin-fixed cow BSE brain. Single-membrane-bound vacuole in an axon terminal. The limiting membrane is detached from adjacent cytoplasm at one pole of the vacuole. *Arrowheads* indicate synaptic vesicles. × 15,000. **b** Mouse inoculated with formalin-fixed kudu brain. Axon terminal showing marked depletion of neurofilaments and microtubules with membranous and granular debris. *Arrowhead* indicates synapse. × 12,000

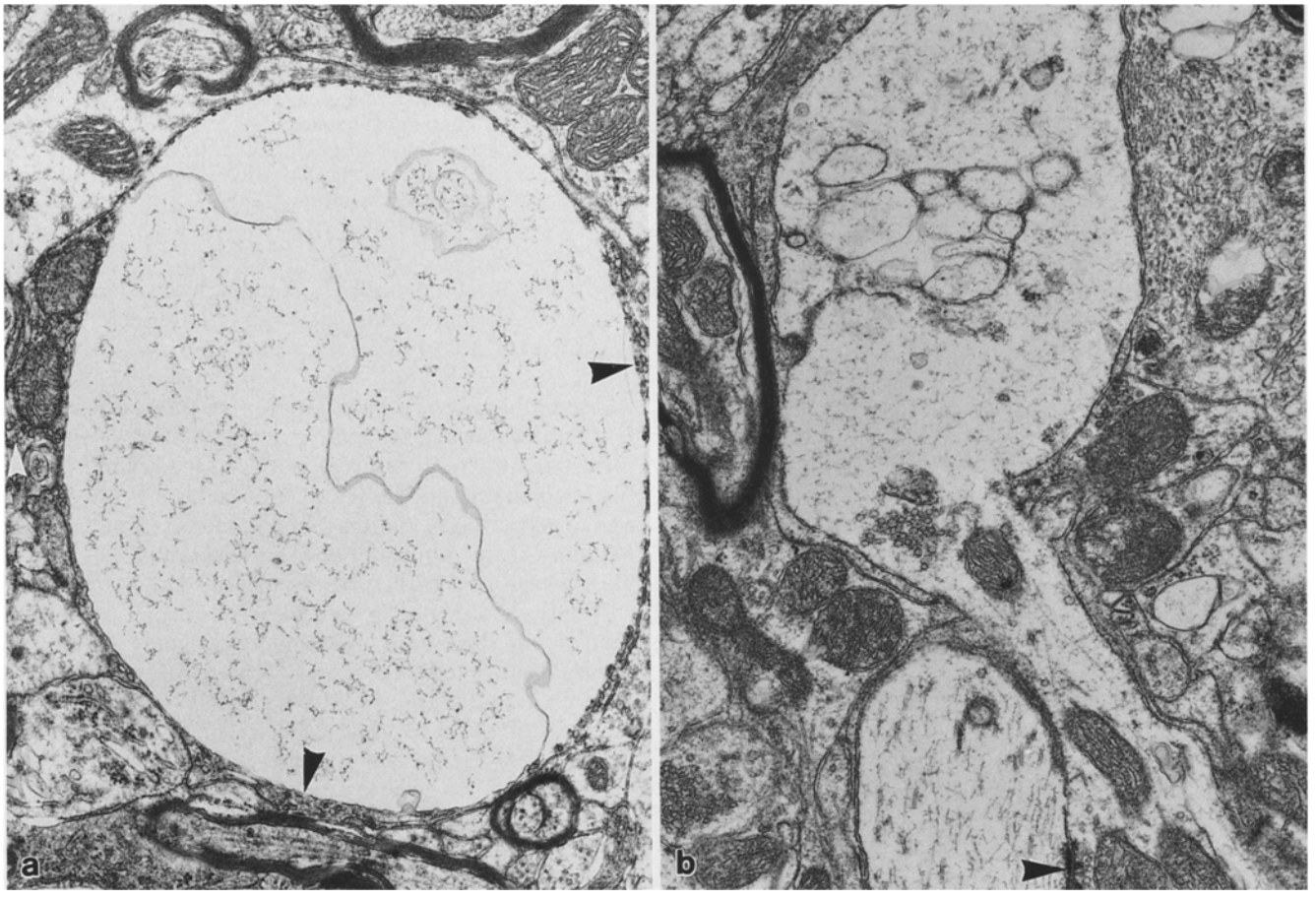

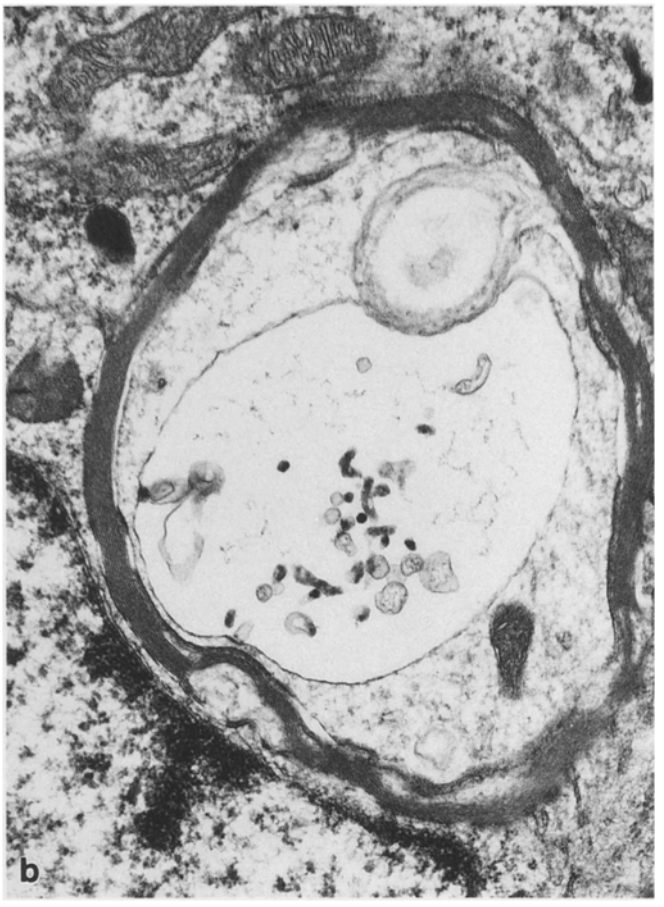

Fig. 4a–c. Vacuoles in myelinated processes. **a** Mouse inoculated with fresh cow BSE brain. Double-membrane-bound vacuole in with membranous and granular debris. × 15,000. **b** Mouse inoculated with formalin-fixed kudu brain. Single-membrane-bound vacuole containing membranous, tubular and vesicular debris. × 24,000. **c** Mouse inoculated with fresh cow BSE brain. Periaxonal vacuole probably located within oligodendrocyte inner tongue. *Asterisk* indicates axon. × 12,500

thy in each infected mouse. The pattern of vacuolation in each of the brains from experimentally inoculated mice is shown in Table 1.

Electron microscopy. Individual mice showed no significant differences in the nature or distribution of primary ultrastructural features irrespective of the bovine species from which the inoculum had been obtained. The nature and distribution of changes seen in mice inoculated with formalin-fixed brain was indistinguishable from that of mice inoculated with fresh brain (Table 1).

Many vacuoles at various stages of development were seen at all sites with light microscopically detectable vacuolation. Numerous large vacuoles were present. It was not usually possible to recognise the cytological location of these vacuoles. Large vacuoles often contained membranous or granular debris although many vacuoles had no visible contents. Large vacuoles had single or no visible limiting membranes. Those with single limiting membranes often had discontinuities of the membrane. Some vacuoles apparently had double

limiting membranes when examined under low magnifications but on closer inspection these were found to be composed of one vacuole membrane with the limiting plasma membrane of a contiguous cell process closely apposed to it. Processes contiguous to large vacuoles were often compressed. Herniation of adjacent cell membranes into the vacuole was also common.

Smaller vacuoles sometimes arose in dendrites (Fig. 2) or axon terminals (Fig. 3). Vacuoles were single membrane bound (Fig. 2b, 3a) or double-membrane bound (Fig. 2c), although some vacuoles did not have a limiting membrane (Fig. 2a). Other vacuoles not recognisably contained within neurites, which were limited by a single unit membrane, were regarded as cell processes. These had few or no remaining microtubules and contained granular or membranous debris. Sometimes recognisable residual subcellular organelles were preserved (Fig. 2d). Several such vacuoles had evidence of synaptic contacts and small numbers of synaptic vesicles were, therefore, defined as axon terminals (Fig. 3b). Classical scrapie-like vacuoles containing membranous or sparse granular material were not seen within neuronal perikarya.

Other vacuoles were seen in myelinated fibres. Some had a similar appearance to the dendritic vacuoles described above (Fig. 4) but other fibres had no recognisable axon within them. Some vacuoles were clearly periaxonal, and were probably present within the oligodendrocyte inner tongue (Fig. 4c). Although some intramyelinic vacuolation was seen, it was only present in fibres showing other degenerative features or vacuolation of the axon or inner tongue.

At some sites, many neuronal perikarya had single- or double-membrane-bound vacuoles containing various cell organelles, dense bodies, amorphous electron-dense material, granular or whorled membranes (Fig. 5). Some larger whorled membrane configurations resembled myeloid bodies. Smaller membrane-bound compartments were present within these vacuoles. The surrounding cytoplasm had a well-developed Golgi apparatus. These structures were interpreted as autophagic vacuoles [3, 4]. Many neurons contained abundant ceroid-lipofuscin and a progression to lipofuscin-like material could be seen within autophagic vacuoles. A consistent distribution pattern of autophagy was seen (Table 1). The superior colliculus and paraterminal body

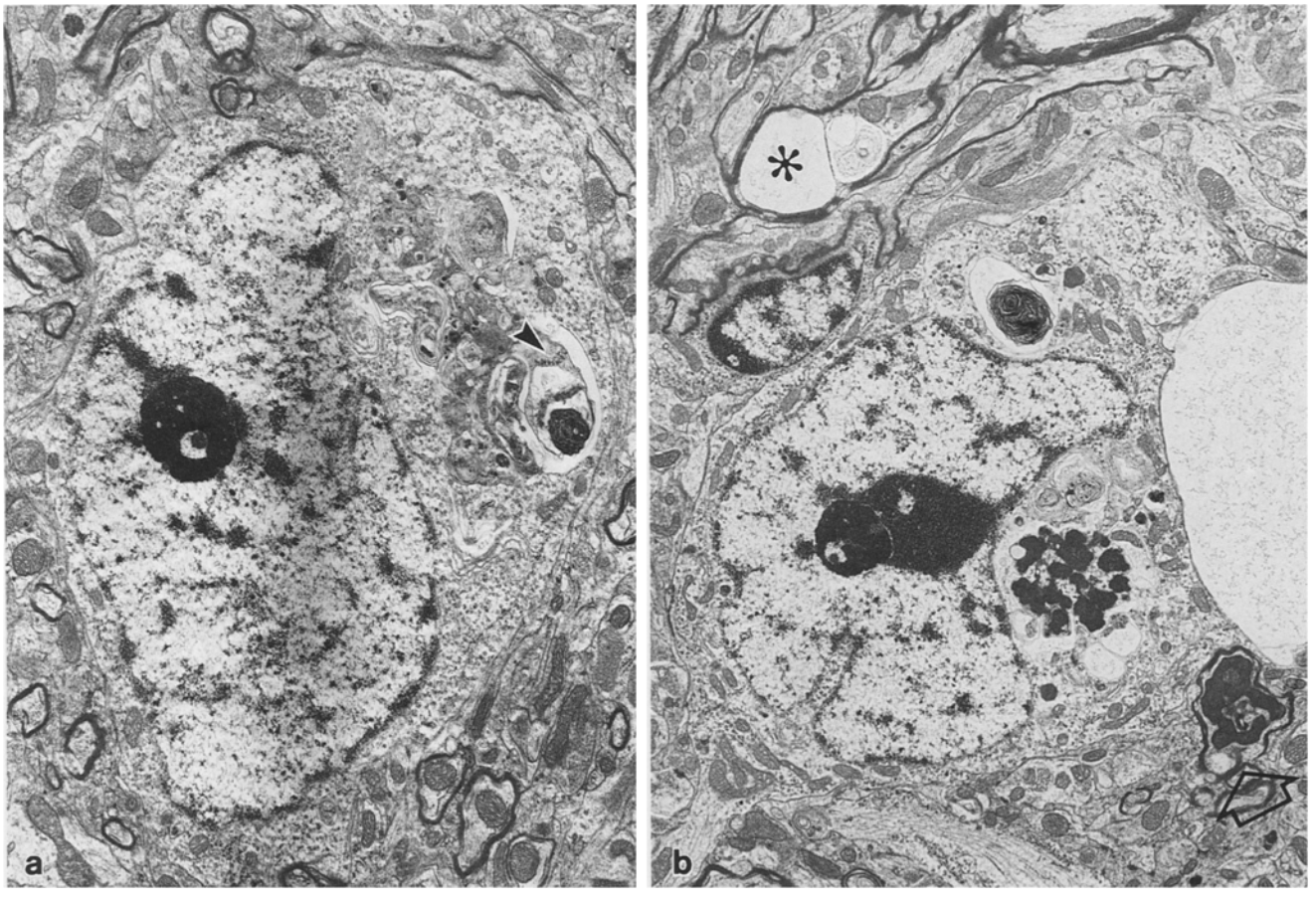

Fig. 5a, b. Mouse inoculated with formalin-fixed nyala brain. Neuronal autophagy. **a** Autophagic vacuoles containing membranous and amorphous electron-dense deposits. Residual ribosomes can be recognised (*arrow*). × 5,100. **b** Several autophagic vacuoles containing granular or membranous material. Electron-dense deposits resembling lipofuscin can also be seen. A large vacuole is adjacent to the neuron. Also present are myelinated fibres showing vacuolation (*asterisk*) and degeneration (*open arrow*). × 5,100

were invariably affected and neurons displaying autophagic features were frequent at these sites. At other sites evidence of autophagy was inconsistent and, when present, only sparse neurons contained autophagic vacuoles. Neuronal autophagy did not, therefore, follow the topographic pattern of vacuolation.

Rare 25- to 30-nm tubular and spherical particles were identified in postsynaptic dendrites and axon terminals. These were characterised as tubulovesicular particles or scrapie-associated particles [2, 9, 32]. Branching tubular structures (Fig. 6b) and, in three mice, unusual paracrystalline bodies composed of membrane stacks were also found (Fig. 6a). Axons containing large numbers of neurofilaments, pleomorphic dense bodies or lysosomes fulfilling the criteria for dystrophic neurites [18] were frequent in all BSE-inoculated mouse brains.

Other changes included axonal swellings filled with mitochondria, neurofilaments and microtubules or vesicular elements. Axonal degeneration and features consistent with Wallerian-type degeneration were also present. As in controls features such as small single-membrane-bound vacuoles, occasional dilated mitochondria and focal, often perivascular, swelling of astrocyte cytoplasm were also present.

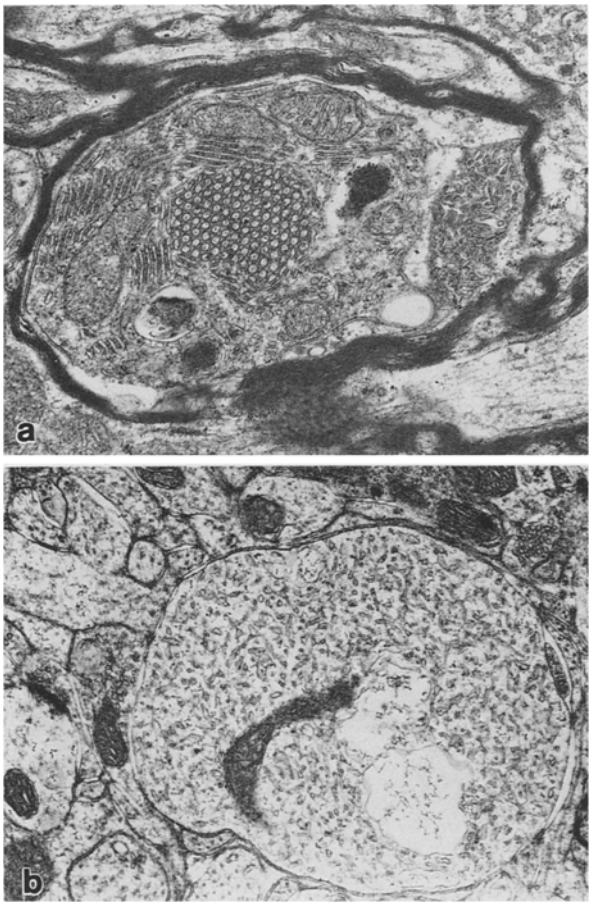

Fig. 6. **a** Mouse inoculated with formalin-fixed nyala brain. Paracrystalline arrays of paired membrane stacks or vesicles in a myelinated process. × 32,000. **b** Mouse inoculated with formalin-fixed cow BSE brain. Interconnecting, branching tubules in a neurite. × 11,000

Discussion

No significant difference in the nature or distribution of vacuolation or ultrastructural findings in mice was seen irrespective of the bovine species from which the inoculum was obtained. This is in contrast to the differing topography of lesions seen in nyala [15], cow [37], and kudu [22]. When compared with inoculum taken from fresh cow brain, formalin-fixed brain inoculum had no significant effect on the lesion distribution or nature of the lesions. These observations support the suggestion that the spongiform encephalopathy observed in small numbers of exotic bovids [10, 15, 22] in wildlife parks in Britain are part of the same epidemic that currently affects cattle [22, 38, 39].

The appearance and cellular location of the vacuoles was similar to that previously described for other transmissible spongiform encephalopathies. Neuronal autophagy was a prominent feature. Neuronal autophagy has been described in experimental scrapie and CJD [3, 4] and increased amounts of ceroid-lipofuscin, an end-product of neuronal autophagy, is also reported in CJD [23].

Considerable controversy exists regarding the precise nature, origin and development of vacuoles. While the consensus view is that vacuolation in the spongiform encephalopathies arises largely in dendrites and also in axons [1, 14, 24, 28, 30–32] some authors suggest that vacuolation may also occur in astrocytes or that swelling of astrocyte processes may contribute to vacuolation [19, 20, 24, 26]. Baker et al. [1] suggested that vacuoles arise from dilated SER. While we agree with these authors that single-membrane-bound vacuoles originating in dendrites and axons are probably derived from SER, such dilated structures are also seen in controls (even in areas which otherwise show good fixation). However, double-membrane-bound vacuoles within neurites and vacuoles thought to originate from loss of subcellular organelles in dendrites could not have arisen from dilated SER.

Studies by Kim and Manuelidis [19, 20] and Lampert et al. [24] described focal clearing of neuronal and glial perikarya and dendrites. We also consider that some of the vacuoles in the present study probably arose from swollen dendrites and are associated with partial or complete loss of organelles. Microtubules appear to be the first organelle lost in this type of vacuole. One of the earliest features of delayed or imperfect fixation is loss of microtubules but dendrites with loss of microtubules or other organelles were located in areas of tissue which otherwise showed criteria for good fixation. It is now commonly recognised that the cytoskeleton plays a fundamental role in the transport of proteins through dendrites and axons. We suggest that this type of vacuole in dendrites and axons, characterised by a loss of organelles, may result from cessation of neurite transport mechanisms with subsequent dissolution or dispersion of microtubules and neurofilaments.

Single- or double-membrane-bound vacuoles located within neurites may, thus, be formed either by the dilation of organelles, such as SER and mitochondria, or

vacuoles may be formed by swelling of cell processes and loss of subcellular organelles. Vacuoles may, therefore, have more than one morphogenesis. However, it is also possible that dilation of SER or double-membrane-bound organelles such as mitochondria may occur as passive expansion of these structures following loss or dispersion of microtubules and other electron-lucent components of neurites, perhaps as a result of decreased or arrested axonal transport mechanisms. Such an explanation does not, however, adequately explain periaxonal vacuolation or previous accounts of vacuolation in myelin [28, 30, 33].

Some of the vacuoles in myelinated fibres had no visible axon and others were located in oligodendrocyte inner-tongue cytoplasm. Several of the smaller vacuoles within myelinated fibres lacking axons were probably associated with Wallerian-type degeneration and subsequent digestion of the axon. Similar though fewer vacuoles occurred in controls where low frequency axonal and Wallerian-type degeneration was also present.

Brains from animals and man terminally affected with transmisible-spongiform encephalopathies show, in addition to grey matter vacuolation, evidence of other pathological processes. These include Wallerian-type degeneration [11], astrocytosis [25, 26, 30], neuronal autophagy [3, 4], macrophage infiltration and intramyelinic vacuoles [28, 33]. The relative frequency of each of these components in experimental animals depends on the strain of the infecting agent and host genotype. In view of these extensive and varied pathological responses and the probable multiple morphogeneses of vacuoles, we think it likely that vacuolation may arise by a number of mechanisms and that an impending total breakdown of homeostatic mechanisms in neurons may give rise to spongiform changes of a non-specific nature, perhaps largely mediated by failure of axonal transport mechanisms. Slow axonal transport is implicated in the spread of scrapie infectivity within the CNS [21, 34]. Control brains show the same range of vacuoles with similar features which supports the suggestion that vacuoles in scrapie-like diseases may not be disease specific but may relate to the acceleration of homeostatic or physiological degenerative processes. Thus, the low levels of specific scrapie-like vacuolation seen in the early stages of incubation of scrapie cannot invariably be distinguished from vacuolation in controls [16]. Vacuolation recognisable as diagnostic or specific for scrapie-like disease tends to occur quite abruptly and is based on the frequency rather than the form of the vacuoles. In serial studies vacuolation usually increases markedly as clinical disease approaches [16, 20].

When comparing observations reported in different ultrastructural studies there is always the concern that small differences in the fixation or processing methods used give rise to artefacts which may accentuate or introduce apparent pathological changes. There are many inconsistencies in the descriptions of vacuolation in the spongiform encephalopathies and while some of the reported findings have been considered to be artefactual [13] other differences are not so readily dismissed. Several studies describe vacuolation of myelin [28, 30, 33] (particularly when CJD sources of inoculum are used), while other studies suggest that neuronal perikaryal vacuolation is frequent [24, 25, 32]. In two studies of CJD in guinea pigs, vacuolation of neuronal nuclei was considered a pathological feature [19, 20]. Vacuolation of myelin (other than that associated with degenerate axons), neuronal perikaryal vacuolation and nuclear vacuolation were absent in the present study. This may be explained by genuine strain differences in agent or host responses to infection.

Scrapie-associated particles or tubulovesicular particles and dystrophic neurites are also previously reported features of the transmissible spongiform encephalopathies [2, 9, 27, 29, 31]. Both of these features, as well as processes containing branching tubules and other novel particles, were found in this study. Tubulovesicular particles are inconsistent features of transmissible spongiform encephalopathies [15, 24] but are not described for other degenerative encephalopathies of animals or man. Descriptions of their morphology are rather diverse [2, 9, 13, 29]. The diameter of tubulovesicular bodies approximates to that of microtubules and it has been suggested that they may be formed from the degeneration of such organelles [13]. Dystrophic neurites are non-specific structures found in control brains as well as occurring following toxic and traumatic insults [18]. Branching tubules in processes may also be found in control rodent brains (M. Jeffrey, personal observations). We consider dystrophic neurites and branching tubules to be epiphenomena because of their occurrence in controls and/or other toxic disorders. Similarly tubulovesicular bodies are probably not significant in the pathogenesis of scrapie because they occur inconsistently and are morphologically diverse.

Autophagy, the process of sequestration and subsequent digestion of a damaged portion of cytoplasm following local intracellular injury, is a well-known indicator of catabolic activity. In this process a damaged portion of cytoplasm is linked to autophagosomes or lysosomes and digested. The end product of autophagy is thought to be lipofuscin. In vitro studies of scrapie-infected murine cells have shown that the biosynthesis of the normal protease-sensitive isoform of prion protein (PrP^c) begins in the ER and is processed through the Golgi apparatus from where it is moved to the cell surface [7]. PrP^{sc} (the protease-resistant isoform) is synthesized and degraded much more slowly than PrP^c [7] and it is formed in the biosynthetic cycle after it reaches the cell surface or at some later point in the metabolic pathway [6]. In these scrapie-infected cells PrP^{sc} is first metabolised in endosomes and early lysosomes [7, 8, 36] and accumulates intracellularly [7, 35, 36]. We suggest that frequent autophagosomes seen in neurons of BSE-affected mice are morphological indications of functional lysosomal and endosomal perturbations caused by the excessive accumulation and metabolism of PrP^{BSE}. In previous studies of naturally occurring BSE in cattle we have shown that the 1B3 antiserum for PrP reacts with ceroid-lipofuscin in controls and BSE-affected brains [17]. Furthermore, we

have shown that severe neuronal loss, which does not correlate with the severity of vacuolation, and which is unsuspected by routine light microscopic methods, is present in BSE cow brains [17]. We, therefore, also suggest that excess accumulation of PrP following infection with scrapie or BSE agent may result in excess catabolic activity visible by electron microscopy as autophagy and by optical and electron microscopy as excess accumulation of lipofuscin. Continued accumulation of PrP results in repeated autophagic events and ultimately neuronolysis and neuronal loss.

Putative PrP^{sc} accumulation in lysosomes of neurons in vitro does not explain the widespread and locally intense distribution of PrP^{sc} in neuropil reported by light microscope studies of murine scrapie [5]. As many such areas of neuropil are composed largely of neurites which have few lysosomes, PrP^{sc} cannot be entirely located to lysosomes in vivo. The relationship between PrP^{sc} accumulation and morphological pathological changes awaits the accurate ultrastructural localisation of PrP^{sc} in vivo.

References

1. Baker HF, Duchen LW, Jakobs JM, Ridley RM (1990) Spongiform encephalopathy transmitted experimentally from Creutzfeldt-Jakob and familial Gerstmann-Sträussler-Scheinker diseases. Brain 113:1891–1909
2. Baringer JR, Prusiner SB, Wong JS (1981) Scrapie-associated particles in post-synaptic particles in post-synaptic processes. Further ultrastructural studies. J Neuropathol Exp Neurol 40:281–288
3. Boellaard JW, Schlote W, Tateishi J (1989) Neuronal autophagy in experimental Creutzfeldt-Jakob's disease. Acta Neuropathol 78:410–418
4. Boellaard JW, Kao M, Schlote W, Diringer H (1991) Neuronal autophagy in experimental scrapie. Acta Neuropathol (Berl) 81:225–228
5. Bruce ME, McBride PA, Farquhar CF (1989) Precise targeting of the pathology of the sialoglycoprotein, PrP, and vacuolar degeneration in mouse scrapie. Neurosci Lett 102:5–15
6. Caughey B, Raymond GJ (1991) The scrapie-associated form of PrP is made from a cell surface precursor that is both protease and phospholipase sensitive. J Biol Chem 266:18217–18223
7. Caughey B, Race RE, Ernst D, Buchmeier HH, Chesebro B (1989) Prior protein (PrP) biosynthesis in scrapie infected and uninfected neuroblastoma cells. J Virol 63:175–181
8. Caughey B, Raymond GJ, Ernst D, Race RE (1991) N-terminal truncation of the scrapie-associated form of PrP by lysosomal protease(s): implications regarding the site of conversion of PrP to the protease-resistant state. J Virol 65:6597–6603
9. David-Ferreira JF, David-Ferreira KL, Gibbs CJ (1968) Scrapie in mice: ultrastructural observations in the cerebral cortex. Proc Soc Exp Biol Med 127:313–320
10. Fleetwood AJ, Furley CW (1990) Spongiform encephalopathy in an eland. Vet Rec 126:408
11. Fraser H (1969) The occurrence of nerve fibre degeneration in brains of mice inoculated with scrapie. Res Vet Sci 10:338–341
12. Fraser H, McConnell I, Wells GAH, Dawson H (1988) Transmission of bovine spongiform encephalopathy to mice. Vet Rec 123:472
13. Gibson PH, Doughty LA (1989) An electron microscopic study of inclusion bodies in synaptic terminals of scrapie-infected animals. Acta Neuropathol 77:420–425
14. Gray EG (1986) Spongiform encephalopathy: a neurocytologist's viewpoint with a note on Alzheimer's disease. Neuropathol Appl Neurobiol 12:149–172
15. Jeffrey M, Wells GAH (1988) Spongiform encephalopathy in a nyala (*Tragelaphus angasi*). Vet Pathol 25:398–399
16. Jeffrey M, Scott JR, Fraser H (1991) Scrapie inoculation of mice: light and electron microscopy of the superior colliculi. Acta Neuropathol 81:562–571
17. Jeffrey M, Halliday WG, Goodsir CM (1992) A morphometric and immunohistochemical study of the vestibular nuclear complex in bovine spongiform encephalopathy. Acta Neuropathol (in press)
18. Jellinger K (1973) Neuroaxonal dystrophy: its natural history and related disorders. Neuropathol 2:129–180
19. Kim JK, Manuelidis EE (1983) Ultrastructural findings in experimental Creutzfeldt-Jakob disease in guinea pigs. J Neuropathol Exp Neurol 42:29–43
20. Kim JK, Manuelidis EE (1986) Serial ultrastructural study of experimental Creutzfeldt-Jakob disease in guinea pigs. Acta Neuropathol (Berl) 69:81–90
21. Kimberlin RH, Walker CA (1982) Pathogenesis of mouse scrapie: patterns of agent replication in different parts of the CNS following intraperitoneal infection. J R Soc Med 75:618–624
22. Kirkwood JK, Wells GAH, Wilesmith JW, Cunningham AA, Jackson SI (1990) Spongiform encephalopathy in an arabian oryx (*Oryx leucoryx*) and a greater kudu (*Tragelaphus strepsiceros*). Vet Rec 127:418–420
23. Kirschbaum WR (1968) Creutzfeldt-Jakob disease. Elsevier, New York, pp 210–228
24. Lampert PW, Earle KM, Gibbs CJ, Gajdusek DC (1969) Experimental kuru encephalopathy in chimpanzees and spider monkeys. Electron microscope studies. J Neuropathol Exp Neurol 28:353–370
25. Lampert PW, Hooks J, Gibbs CJ, Gajdusek DC (1971) Altered plasma membranes in experimental scrapie. Acta Neuropathol (Berl) 19:81–93
26. Landis DMD, Williams RS, Masters CL (1981) Golgi and electron microscopic studies of spongiform encephalopathy. Neurol 31:538–549
27. Liberski PP, Yanagihara R, Gibbs CJ, Gajdusek DC (1989) Scrapie as a model for neuroaxonal dystrophy: ultrastructural studies. Exp Neurol 106:133–141
28. Liberski PP, Yanagihara R, Gibbs CJ, Gajdusek DC (1989) White matter ultrastructural pathology of experimental Creutzfeldt-Jakob disease in mice. Acta Neuropathol 79:1–9
29. Liberski PP, Yanagihara R, Gibbs CJ, Gajdusek DC (1990) Appearance of tubulovesicular structures in experimental Creutzfeldt-Jakob disease and scrapie preceeds the onset of clinical disease. Acta Neuropathol 79:349–354
30. Liberski PR, Yanagihara R, Asher DM, Gibbs CJ, Gajdusek DC (1990) Re-evaluation of the ultrastructural pathology of experimental Creutzfeldt-Jakob disease. Serial studies of the Fuujisaka strain of Creutzfeldt-Jakob disease virus in mice. Brain 113:121–127
31. Narang HK (1974) An electron microscopic study of natural scrapie sheep brain: further observations on virus-like particles and paramyxovirus-like tubules. Acta Neuropathol (Berl) 28:317–329
32. Sasaki S, Mizoi S, Akashima A, Shinagawa M, Goto H (1986) Spongiform encephalopathy in sheep scrapie: electron microscopic observations. Jpn J Vet Sci 48:791–796
33. Sato Y, Ohta M, Tateishi J (1980) Experimental transmission of human subacute spongiform encephalopathy to small rodents. II. Ultrastructural study of spongy state in the grey and white matter. Acta Neuropathol (Berl) 51:135–140

34. Scott JR, Fraser H (1989) Enucleation after intraocular scrapie injection delays the spread of scrapie. Brain Res 504:301–305
35. Taraboulos A, Serban D, Prusiner SB (1990) Scrapie prion proteins accumulate in the cytoplasm of persistently infected cultured cells. J Cell Biol 110:2117–2132
36. Taraboulos A, Borchelt DR, McKinley MP, Raeber A, Serban D, Prusiner SB (in press). Pathway of PrP^{sc} biosynthesis in cultured cells. In: Prusiner SB, Collinge J, Powell J, Anderton B (eds) Prion diseases of humans and animals. Ellis Horwood, Hemel Hempstead
37. Wells GAH, Wilesmith JW, McGill IS (1991) Bovine spongiform encephalopathy: a neuropathological perspective. Brain Pathol 1:69–78
38. Wilesmith JW, Wells GAH, Cranwell MP, Ryan JBM (1990) Bovine spongiform encephalopathy: epidemiological studies. Vet Rec 123:638–644
39. Wilesmith JW, Ryan JBM, Atkinson MJ (1991) Bovine spongiform encephalopathy: epidemiological studies on the origin. Vet Rec 128:199–203